Final version available at Elsevier : http://dx.doi.org/10.1016/j.sna.2014.02.030

Al-Al thermocompression bonding for wafer-level MEMS sealing

N. Malik [a,b], K. Schjølberg-Henriksen [b], E. Poppe [b], M.M.Visser Taklo [c] and T.G. Finstad [a]
[a] *Centre for materials science and nanotechnology, University of Oslo, Oslo, Norway*
[b] *SINTEF ICT, Dept. of Microsystems and Nanotechnology, P.O. Box 124 Blindern, N-0314 Oslo, Norway*
[c] *SINTEF ICT, Dept. of Instrumentation, P.O. Box 124 Blindern, N-0314 Oslo, Norway*

K. Schjølberg-Henriksen: Kari.Schjolberg-Henriksen@sintef.no
E. Poppe: Erik.Poppe@sintef.no
M.M.Visser Taklo: Maaike.Taklo@sintef.no
T.G. Finstad: terje.finstad@fys.uio.no
Corresponding Author:
*Nishant Malik, Postboks 1048, Blindern, 0316, Oslo, Norway, + 47 463 50 668, nishant.malik@smn.uio.no

ABSTRACT

Al–Al thermocompression bonding has been studied using test structures relevant for wafer level sealing of MEMS devices. Si wafers with protruding frame structures were bonded to planar Si wafers, both covered with a sputtered Al film of 1 µm thickness. The varied bonding process variables were the bonding temperature (400 °C, 450 °C and 550 °C) and the bonding force (18, 36 and 60 kN). Frame widths 100 µm, 200 µm, with rounded or sharp frame corners were used. After bonding, laminates were diced into single chips and pull tested. The effect of process and design parameters was studied systematically with respect to dicing yield, bond strength and resulting fractured surfaces. The test structures showed an average strength of 20-50 MPa for bonding at or above 450 °C for all three bonding forces or bonding at 400 °C with 60 kN bond force. The current study indicates that strong Al-Al thermocompression bonds can be achieved either at or above 450 °C bonding temperature for low (18 kN) and medium (36 kN) bond force or by high bond force (60 kN) at 400 °C. The results show that an increased bond force is required to compensate for a reduced bonding temperature for Al-Al thermocompression bonding in the studied temperature regime.

HIGHLIGHTS

- Al-Al thermocompression bonding was demonstrated at a temperature as low as 400 °C. High dicing yield was achieved by applying a high bond force of 60 kN.
- The possibility of reducing the bond force to 18 kN was demonstrated. The reduction in bond force required an increase in the bonding temperature to 450 °C.
- Cohesive fracture in the bulk silicon below the Al layers was observed to a large extent, indicating good adhesion between Si and Al, and strong Al-Al bonded interfaces.

KEYWORDS

Metal bonding, Aluminum, MEMS, Thermocompression bonding, Bond force, Dicing yield, Cohesive Si fracture, Bond strength.

1. INTRODUCTION

Micro electromechanical systems (MEMS) typically contain moveable parts which complicate handling during packaging. A so-called zero level packaging step is therefore introduced for several MEMS products. Wafer-level sealing is targeted for large volume MEMS products due to superior throughput with related cost efficiency and potentially high reproducibility of good quality seals [1].

A wide range of wafer-level sealing methods, or bonding techniques, exists. Among the variety of techniques, anodic bonding, adhesive bonding, glass frit bonding, and high-temperature or surface activated silicon direct bonding are commonly used [2]. However, each bonding technique has its limitations and requirements regarding wafer surface, bonding temperature, electric field application, and minimum bondable feature size. Thermocompression bonding using deposited metal films as bonding material is promising for wafer-level encapsulation. Metals such as Au [3, 4], Cu [4, 5] and Al [4, 6-9] have been demonstrated as bonding layer between two silicon wafers. Bonding with an intermediate metallic layer is an attractive choice for MEMS devices. Fraux [10] reports that the company STMicroelectronics shrunk

the size of their accelerometers by 57% when using Au-Au thermocompression bonding instead of glass-frit bonding. At the company Analog Devices, bond frames as narrow as 10 µm have been investigated for Al-Al thermocompression bonding [9]. Farrens [11] shows that a seal of a certain width can sustain a hermetic seal for a longer time when it is sealed by a metal than by glass. Comparing glass and metal seals that are 10µm thick, the lifetime of the glass seal is a few years versus a century or more for the metal seal [11]. Additionally, the good electrical and thermal conductivity properties of a metal based seal can be exploited in a MEMS design by adding e.g. electrical interconnects or thermal shorts.

In thermocompression bonding, metallic bonds are formed between metal deposited substrates by bringing them into intimate contact and simultaneously applying temperature and pressure [4]. The applied pressure must be high enough to bring the surfaces into atomic contact despite any surface roughness. The technique is also sometimes called diffusion bonding [11].

Among different metals, Al is especially attractive because of its CMOS compatibility. Successful Al thermocompression bonding has been reported, but only limited details of bonding parameters for wafers having patterned bonding area have been presented [4, 6-9]. Yun *et al.* bonded wafers by applying a range of bond forces for Al films with a range of Cu impurity levels (0% to 4%). They studied the effect of the different parameters on yield and shear strength of diced chips. The highest yield was reported for pure Al whereas the highest shear strengths were reported for the maximum tested impurity level of Cu [7]. Dragoi *et al.* investigated the effect of varying bonding temperature and the effect of various environments for Al-Al thermocompression bonding. A bond tool pressure of 3.4 MPa was applied. A 500nm thick layer of Al (1% Si) sputtered on blanket Si wafers was used as bonding layer. No effect on the bond quality could be observed for any of the tested environments. However, a trend of improved bond interface quality with increasing bonding temperature was reported [6].

The present investigation is a systematic study of various frame designs, bonding temperature and pressure dependence of Al–Al thermocompression bonding using pure (99.999 %) Al films. Test structures suitable for wafer level encapsulation of MEMS devices were used.

2. EXPERIMENTAL

As shown in Fig. 1, Al sputtered plain Si wafers (150 mm) were bonded to Al sputtered Si wafers with 6 µm high protruding bond frames. Three different geometries of bond frames were designed. The bond frames were either 100 µm or 200 µm wide and had either square or rounded corners, see Fig. 2 and Table 1. The total bonding area on the wafer was 525 mm^2. Each structure spanned an area of 3×3 mm^2 and the size of each chip was 6×6 mm^2.

The protruding Si frames were realized by deep reactive ion etching (DRIE) applying an AMS200 I-Productivity etcher (Alcatel) and SiO_2 as masking material. RCA cleaning ending by a 10 s HF dip was done on all wafers before sputtering of Al. A back sputter etch was included to ensure cleanliness and a complete removal of native oxide from the wafers. A layer of 1 µm thick pure Al (99.999 %) was deposited on all wafers to be bonded. The roughness of the deposited Al layer was measured using a Zygo New view™6300 white light interferometer.

Wafer laminates were made by bonding plain and patterned wafers together in an EVG®510 bonder. The bonding time (60 min) and the bonding atmosphere (<1e-3 mbar) were kept constant in the bonding experiments whereas the bonding temperature and the bond force were varied. The bonding temperature was set to 400 °C, 450 °C, or 550 °C. The bonding force was set to 18 kN (low), 36 kN (medium), or 60 kN (high). The applied forces corresponded to bond pressures of 34.28 MPa, 68.57 MPa, and 114.3 MPa, respectively. An overview of the bonded laminates is found in Table 2. The wafers were loaded into the bond chamber, separated with mechanical spacers. After a pump-down to the desired vacuum level, the temperature was raised to the desired value, the spacers were removed, and the tool force was applied. The tool force was kept constant during the 60 min of bonding at the bonding temperature. During the subsequent cool down, the tool force was reduced to 1 kN and kept at this level until the bond temperature was below 50 °C.

After bonding, the laminates were diced into individual dies by a diamond saw. The dicing yield, defined as the percentage of dies that were not delaminated after the dicing process, was recorded. The bond strength was measured by pull testing bonded dies. A random selection of 12 non delaminated dies was made from each laminate, glued to flat headed bolts and pull tested using a MiniMat2000 (Rheometric Inc.). It should be noted that before the random selection of dies for pull testing, there was a "pre-selection" of dies through the dicing process. During pull testing, elongation versus applied force was recorded and the force, at which the fracture occurred, designated as the fracture force, was noted. The bond strength was calculated by dividing the fracture force by the bonding area listed in Table 1. The fractured surfaces of the pull-tested dies were studied and characterized by optical microscopy. The percentage of the nominal bonding area having a cohesive fracture in the bulk silicon was estimated for each die, and designated as the

cohesive fracture number (CFN). A differentiation between cohesive fracture inside the Al and fractures at the Si-Al or Al-Al interfaces was not attempted.

3. RESULTS

The roughness of the sputtered Al layers was approximately 1.5 nm (rms) for both plain and structured wafers as measured on the surfaces to be bonded.

The dicing yield results of the bonding experiments performed for the tested low bond force (18 kN) at different temperatures are presented in Fig. 3. A trend of increased dicing yield with increased temperature was observed. The dicing yield was above 80 % for the bonding temperatures 450 °C and 550 °C. The dicing yield results for the tested medium bond force (36 kN) are presented in Fig. 4. It was observed that the dicing yield for all frame designs was below 40 % at 400 °C, but almost 100 % at 450 °C and 550 °C. A steep increase in dicing yield was thus noticed when going from a bonding temperature of 400 °C to 450 °C at low or medium bond force. Experiments were also conducted using a high (60 kN) bond force. The results are presented in Fig. 5 where the dicing yield of laminates bonded at 400 °C, applying a low, medium or high bond force, are compared. The dicing yield of all bond frame designs was below 47 % for the low or medium bond forces and above 77% for the high bond force. A steep increase in dicing yield was thus noticed when increasing the bond force from medium to high at 400 °C.

Typical fracture surfaces from pull tests performed on single dies of design F200R are presented in Fig. 6. A typical appearance of the fracture surfaces for all tested temperatures and bond forces are included. The dark grey colored parts at or near the fractured bond frames were defined as cohesive fracture in the bulk silicon. Some of these regions have also been studied with SEM with EDS to confirm that the fracture surface was indeed Si. Higher magnification also revealed a surface that is typical for fracture of crystalline Si. Further, these regions were protruding on one side of a fractured surface of a delaminated die while was showing an inverted topography on the opposing surface of the delaminated die , further assuring the cohesive Si fracture nature of the dark grey regions in Fig. 6. White and shiny regions at the fractured bond frames were concluded to correspond to either adhesive fracture at the Al-Al interface, or cohesive fracture in the Al. A differentiation between these latter possibilities was not attempted.

Cohesive fracture numbers (CFN) are plotted in Figs. 7 and 8 for low and medium bond force. The error bars in the Figures represent the standard deviation of the measurements. Even if the error bars were large, a trend of increased CFN with increased temperature was observed. The average CFN was above 80 % for wafers bonded at 550 °C for both low and medium bond force. The CFN for wafers bonded at 400 °C with low, medium and high bond force is presented in Fig. 9. It shows a trend of increased CFN with increased bond force.

The results of the pull test measurements are shown in Fig. 10 (low bond force, all temperatures), Fig. 11 (medium bond force, all temperatures), and in Fig. 12 (400 °C, all bond forces). The error bars represent the standard deviation of the measured values. The standard deviations were to some extent larger than the differences between the data points. The value of bond strength was between 10-50 MPa for all dies, irrespective of bond parameters and frame types. No correlation was found between CFN and bond strength for individual dies.

4. DISCUSSION

The bond force and the bonding temperature were the key experimental variables for obtaining a strong bond. Based on the observed dicing yield in particular, there were clear trends and indicators for which part of the parameter space could give a strong bond and which parts were much less favorable. As expected, and for reasons we present below, the bonding improves with increasing bonding temperature and bonding force. Regarding the less favorable parameter space, as seen in Figs. 3, 4 and 5, the dicing yield was below 50 % for bonding at low and medium bond force at 400 °C for all frame designs. Such low value is defined as poor bonding quality and is assumed to indicate incomplete bonding. The dicing yield increased with increasing bond temperature. At 450 °C, high dicing yield was obtained while at 550 °C almost 100 % dicing yield was obtained for both low and medium bond forces, indicating strong bonding. For applications the bond has to be strong enough to withstand dicing and packaging process steps. Furthermore, the bonding has to ensure good protection of the device during the lifetime. Knechtel has reported that a fracture load of 20 MPa was sufficient for most applications [12]. As seen from Figs. 10, 11 and 12, the laminates that showed high dicing yield also had acceptable bond strength for industrial purposes. The acceptable parameter space could be extended to include bonding at 400 °C by applying high bonding force, which we consider promising for low temperature bonding. There was no significant difference in dicing yield for the three different designs F100, F200 and F200R.

Our result is in agreement with the result of Yun *et al.*, who reported a high dicing yield at a bonding temperature of 450 °C [7]. The observed increase in bond quality with increasing bonding temperature is similar to the results reported

by Dragoi *et al*. [6]. However, in our study, 450 °C seemed to be a sufficiently high bonding temperature, while Dragoi *et al*. reported a threshold temperature between 450 °C and 500 °C. Dragoi *et al*. used 3.4 MPa bond pressure while our lowest bond pressure was 34.28 MPa and the difference in bond pressure could account for the observed difference in threshold temperature.

As seen in Fig. 5, there was a decrease of 10 percentage points in the dicing yield when increasing bond force from low to medium, and an increase of 40 percentage points in dicing yield when increasing the bond force from medium to high. We suggest that the large increase in bond quality with increasing bond force occurred because the high pressure caused excess plastic deformations and helped crush much/more of the Al native oxide. This helped overcoming the surface asperities in the Al film, increasing the area in atomic contact between the two opposing surfaces. Both temperature and pressure applied together assist the bonding between Al-Al surfaces. Figures 3 and 4 show a large increase in dicing yield when increasing the bonding temperature from 400 °C to 450 °C. We think that increasing the temperature enhances the diffusion of metal atoms in the interface region, promoting bonding. Increasing the temperature also softens the material, and further increase the area in atomic contact.

The Figs. 7, 8, and 9 show that the mean CFN was below 50 % for dies bonded at 400 °C while above 80 % for dies bonded at 500 °C. The CFN gives an indication of bond quality, but only to some extent. A high CFN indicates that the strength of Al-Al bond surfaces is stronger that the strength of the crystalline Si in the structure, while a low CFN indicates that this Si is not the weakest material in the structure that is pull tested. The observed trend of the average CFN is that it increased with bond temperature. Both the theory on thermocompression bonding and our dicing yield results could imply an increase in Al-Al bond strength with increasing temperature. If bond strength increased with increasing temperature, an increase in CFN with increasing temperature would also be expected. However, for each individual die in the measurement series, there was no correlation between the CFN and the bond strength measured in the pull test. This fact indicates that the CFN was influenced by other effects in addition to the bond strength of the Al-Al interface. This is further evidenced by the observation that the standard deviation of the measured CFN was larger than the measurement range. Further, even for cases where we assume that we have incomplete bonding (i.e. 400 °C, 18 kN), we observed a high CFN of 80 % for an individual die. Finally, the value of the bond strength was quite low compared the bond fracture strength of Si. These three factors together indicate that CFN is not a simple indicator of bond strength for these measurements and that other factors than the Al-Al interface influence the measurements

Examination of the fractured Si surface after the pull test revealed that he fracture in the bulk Si always occurred at the foot of the protruding Si frame, which is a location for stress concentration in the structure when it is pulled apart. We do not know where the fracture was initiated, but suggest that initiation both in the foot and that the Al-Al interface could result in propagation in bulk Si. We can speculate that process induced defects [13] could have occurred in the test structure which has promoted primary or secondary crack generation at the frame's foot.

5. CONCLUSION

Al-Al thermocompression bonding was investigated in this paper. Three different bond frame designs were bonded at varying bonding temperatures of 400 °C, 450 °C, 550 °C and bond forces of 18 kN, 36 kN and 60 kN. Measurements of dicing yield and the percentage of cohesive fracture in the bulk silicon (CFN) indicate poor bonding at 400 °C and strong bonding at 450 °C and 550 °C for bond forces of 18 kN and 36 kN. Applying 60 kN bond force, a high dicing yield and CFN was obtained also at 400 °C. The measured bond strength was above 20 MPa for dies bonded at temperatures of 450 and 550 °C and for dies bonded at 60 kN. Further studies are necessary to investigate if the bond temperature can be further reduced.

ACKNOWLEDGEMENTS

Financial support from The Research Council of Norway through the project MSENS (Contract No 210601/O30) is gratefully acknowledged.

REFERENCES

[1]M. Esashi, "Wafer level packaging of MEMS", *Journal of Micromechanics and Microengineering*, vol. 18, 2008, 073001. doi:10.1088/0960-1317/18/7/073001

[2]P. Ramm, J.-Q. Lu, M.M.V. Taklo, "Handbook of wafer bonding", *Wiley-vch*, Weinheim, Germany, 2012, pp. 425. doi: 10.1002/9783527644223

[3]M. M. V. Taklo, P. Storås, K. Schjølberg-Henriksen, H. K. Hasting and H. Jakobsen, "Strong, high-yield and low-temperature thermocompression silicon wafer-level bonding with gold" *Journal of Micromechanics and Microengineering*, vol.14, , 2004, pp. 884–890. doi:10.1088/0960-1317/14/7/007

[4]J. Froemel, M. Baum, M. Wiemer, F. Roscher, M. Haubold, C. Jia and T. Gessner, "Investigations of thermocompression bonding with thin metal layers", *Digest Tech. Papers Transducers'11 Conference*, Beijing, China. 5-9 June 2011, pp. 990-993. 10.1109/TRANSDUCERS.2011.5969495

[5]K. N. Chen, C. S. Tan, A. Fan, and R. Reif, "Morphology and Bond Strength of Copper Wafer Bonding", *Electrochemical and Solid-State Letters*, vol.7(1) , 2004, pp. G14-G16. doi: 10.1149/1.1626994

[6]V. Dragoi, G. Mittendorfer, J. Burggraf and M. Wimplinger, "Metal Thermocompression Wafer Bonding for 3D Integration and MEMS Applications", *ECS Transactions at 218th ECS Meeting*, Las Vegas, Nevada, vol. 33(4), October 10-15 2010, pp. 27-35. doi: 10.1149/1.3483491

[7]C. H. Yun, J. Martin, L Chen and T. J. Frey, "Clean and Conductive Wafer Bonding for MEMS", *ECS Transactions at PRIME 2008 International meeting*, Honolulu, Hawaii, vol. 16(8), October 12-17, 2008, pp. 117-124. doi: 10.1149/1.2982860

[8]C.H. Yun, J. R. M., E.B. Tarvin, and J.T. Winbigler, "Al to Al wafer bonding for MEMS encapsulation and 3-D interconnect", *IEEE Papers Micro Electro Mechanical Systems, 2008. IEEE 21st International Conference*, Tucson, AZ, 13-17 Jan. 2008, pp. 810 - 813. doi:10.1109/MEMSYS.2008.4443780

[9]J. Martin, "Wafer capping of MEMS with fab-friendly metals", *Proc. SPIE6463 Reliability, Packaging, Testing, and Characterization of MEMS/MOEMS*, San Jose, CA, vol. 6463, January 19 2007. doi:10.1117/12.701573

[10] R.Fraux, J. Baron, "STMicroelectronics' innovation in wafer-to-wafer bonding techniques shrinks MEMS die size and cost", *3D packaging*, No 21, 2011, pp. 24-27.

[11]S. Farrens, "Metal based wafer level packaging", Suss white paper, 2005. http://www.suss.com/fileadmin/user_upload/technical_publications/WP_WLP_MetalBasedWaferLevelPackaging_0810.pdf

[12]R. Knechtel, "Glass frit bonding: an universal technology for wafer level encapsulation and packaging", *Microsystem Technologies*, vol. 12, 2005, pp. 63–68. doi:10.1007/s00542-005-0022-x

[13] S.A. Campbell, "Fabrication Engineering at the Micro and Nanoscale" 4th edition, *Oxford university Press*, New York, 2013.

FIGURE AND TABLE CAPTIONS

Figure 1: Cross-sectional view of a bonded chip. The top wafer is an Al sputtered plain Si wafer whereas the bottom wafer is an Al sputtered Si wafer with different bond frame designs. The bonded interface is indicated by a dashed line.

Figure 2: Design of the bonding frames called F100, F200 and F200R.

Figure 3: Dicing yield of laminates bonded at 18 kN at different temperatures, calculated for 54 dies of each bond frame design F100, F200, and F200R.

Figure 4: Dicing yield of laminates bonded at 36 kN at different temperatures, calculated for 54 dies of each bond frame design F100, F200, and F200R.

Figure 5: Dicing yield of laminates bonded at 18 kN, 36 kN and 60 kN at 400 °C, calculated for 54 dies of each bond frame design F100, F200, and F200R.

Figure 6: Typical fracture surfaces after pull testing of the F200R bond frame structure for all tested bonding temperatures and bond forces.

Figure 7: Mean and standard deviation of CFN, applying a low bond force of 18 kN, calculated from minimum 9 dies.

Figure 8: Mean and standard deviation of the CFN, calculated from minimum 6 dies. Bond force was 36 kN.

Figure 9: Mean and standard deviation of the CFN, calculated from minimum 10 dies. Bonding temperature was 400 °C.

Figure 10: Mean and standard deviation of the bond strength at bond force of 18 kN, of minimum 9 dies, determined by pull test measurements.

Figure 11: Mean and standard deviation of the bond strength at bond force of 36 kN, of minimum 6 dies, determined by pull test measurements.

Figure 12: Mean and standard deviation of the bond strength at bonding temperature of 400 °C and varying bond forces, of minimum 10 dies, determined by pull test measurements.

Table 1: Description and bonding area of three different types of bond frames.

Table 2: Recipes of all 7 bonded laminates at different temperature and bond forces, all bonded for 60 minutes.

FIGURES AND TABLES

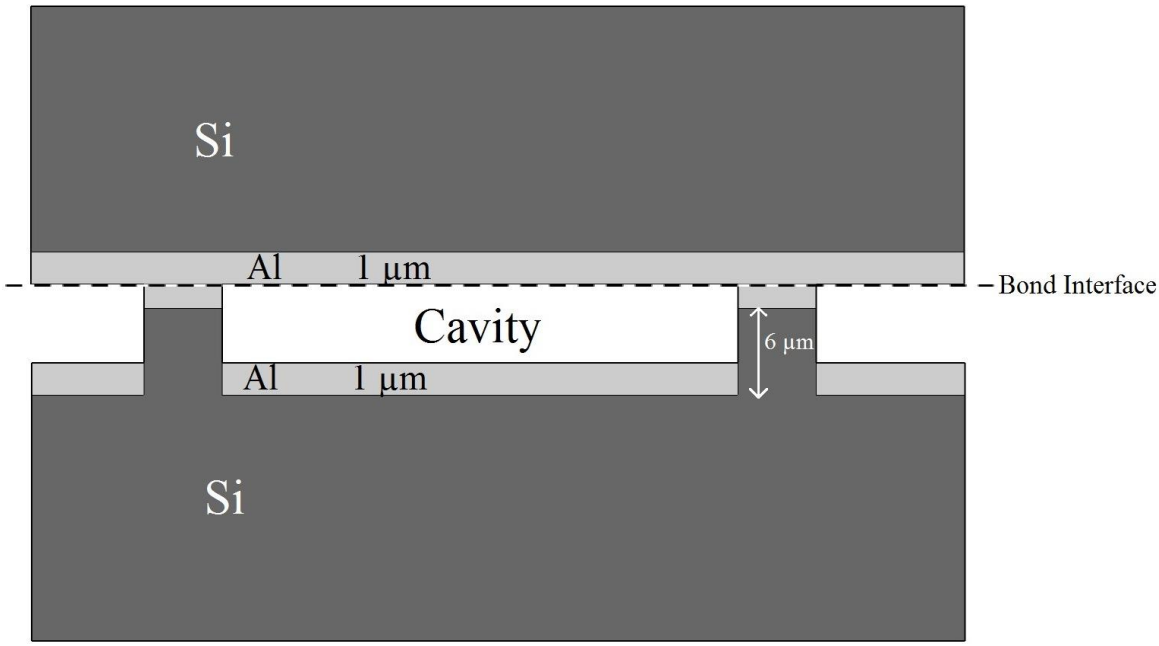

Figure 1: Cross-sectional view of a bonded chip. The top wafer is an Al sputtered plain Si wafer whereas the bottom wafer is an Al sputtered Si wafer with different bond frame designs. The bonded interface is indicated by a dashed line.

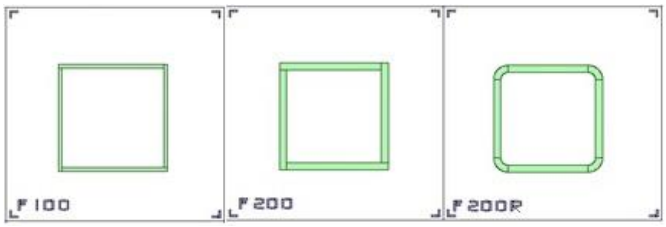

Figure 2: Design of the bonding frames called F100, F200 and F200R.

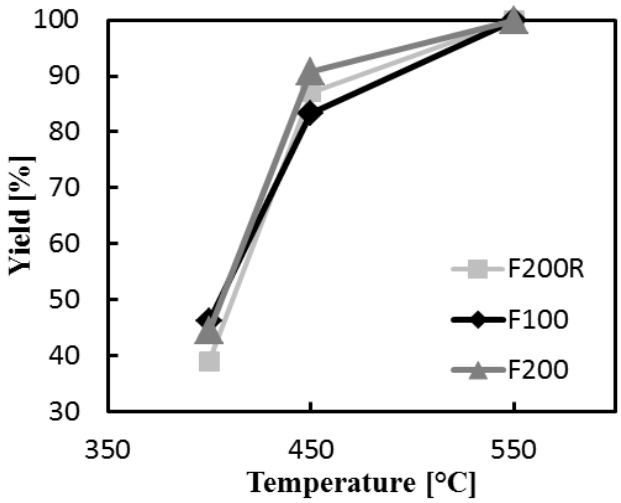

Figure 3: Dicing yield of laminates bonded at 18 kN at different temperatures, calculated for 54 dies of each bond frame design F100, F200, and F200R.

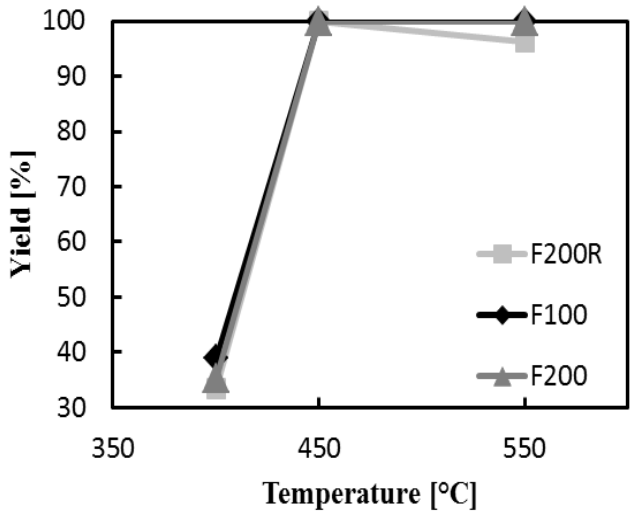

Figure 4: Dicing yield of laminates bonded at 36 kN at different temperatures, calculated for 54 dies of each bond frame design F100, F200, and F200R.

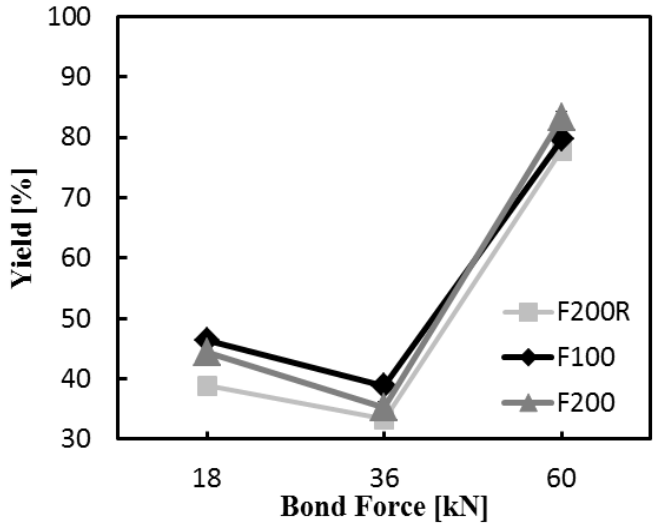

Figure 5: Dicing yield of laminates bonded at 18 kN, 36 kN and 60 kN at 400 °C, calculated for 54 dies of each bond frame design F100, F200, and F200R.

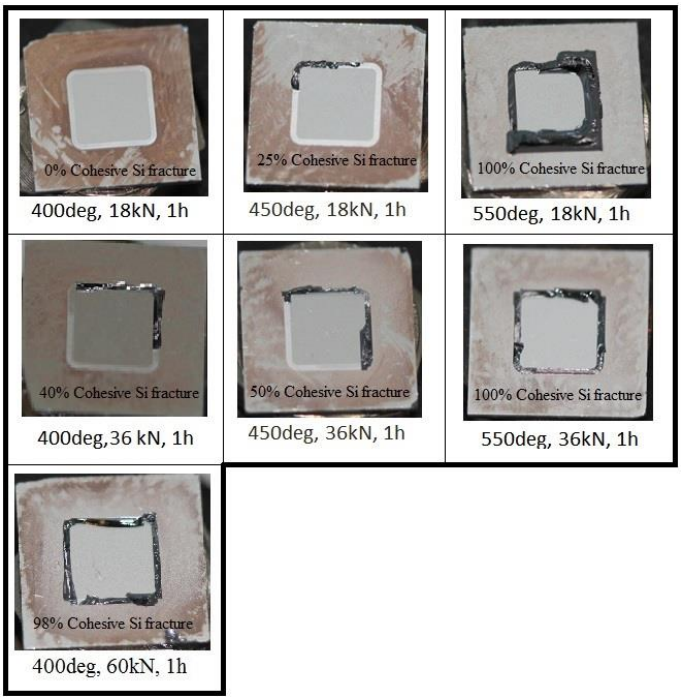

Figure 6: Typical fracture surfaces after pull testing of the F200R bond frame structure for all tested bonding temperatures and bond forces.

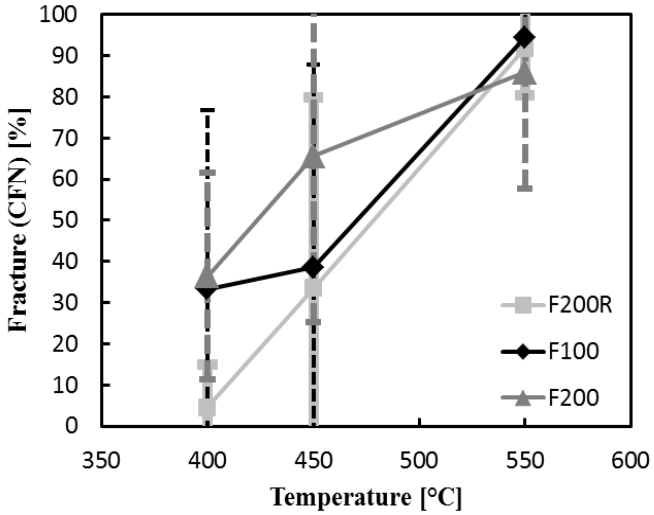

Figure 7: Mean and standard deviation of CFN, applying a low bond force of 18 kN, calculated from minimum 9 dies.

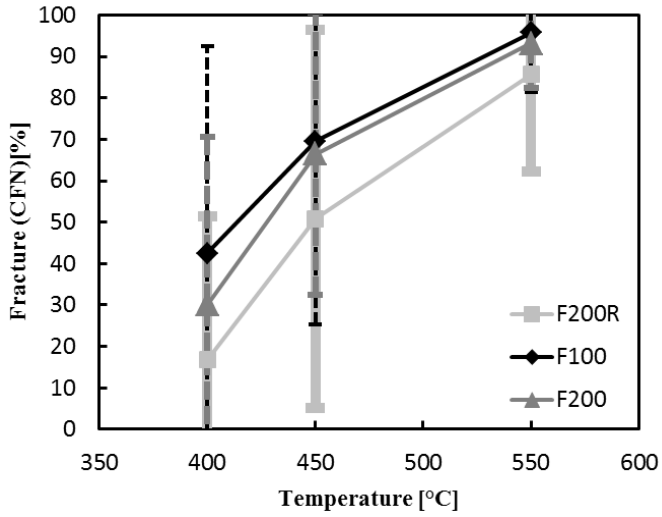

Figure 8: Mean and standard deviation of the CFN, calculated from minimum 6 dies. Bond force was 36 kN.

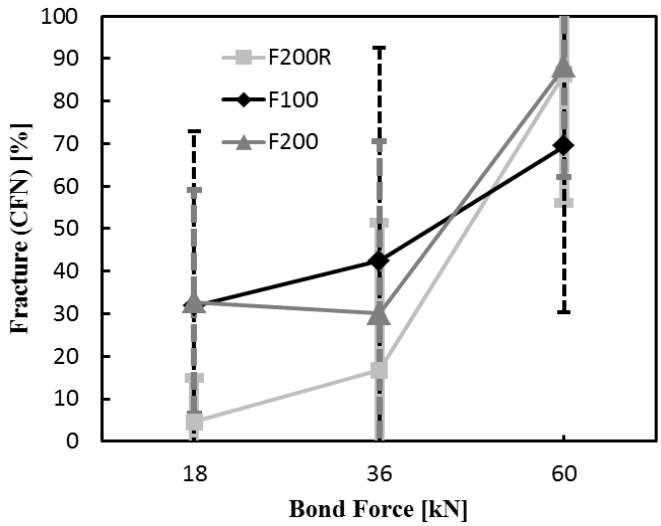

Figure 9: Mean and standard deviation of the CFN, calculated from minimum 10 dies. Bonding temperature was 400 °C.

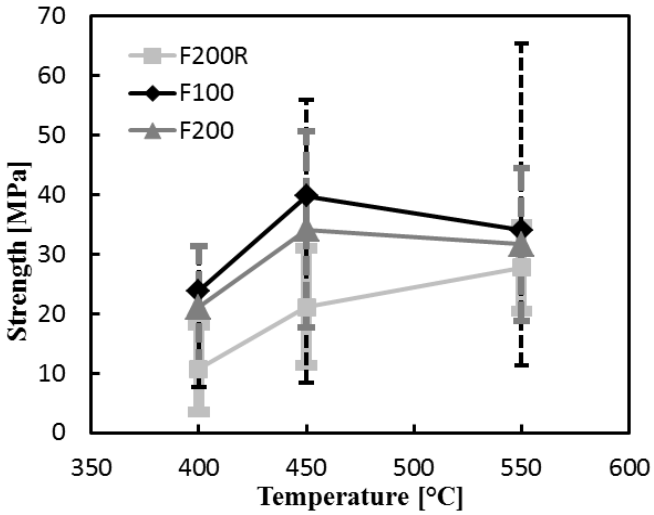

Figure 10: Mean and standard deviation of the bond strength at bond force of 18 kN, of minimum 9 dies, determined by pull test measurements.

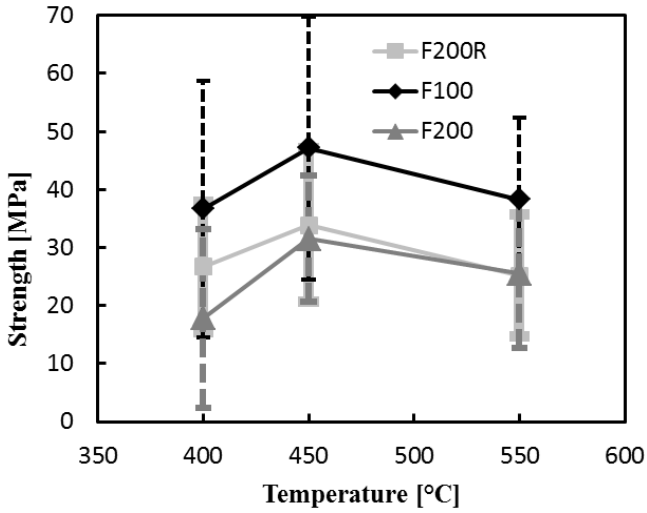

Figure 11: Mean and standard deviation of the bond strength at bond force of 36 kN, of minimum 6 dies, determined by pull test measurements.

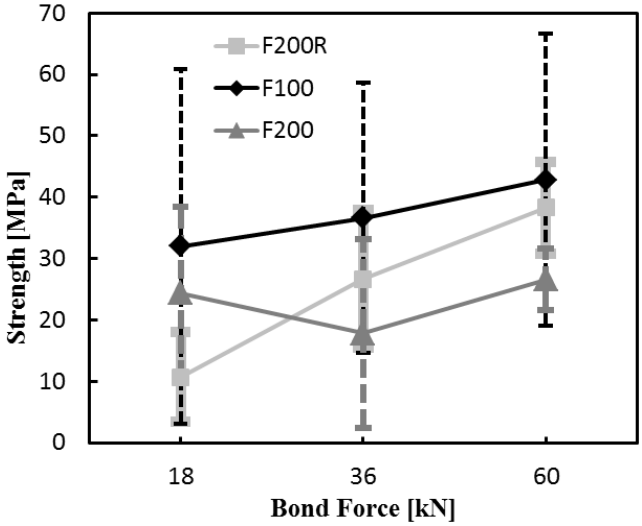

Figure 12: Mean and standard deviation of the bond strength at bonding temperature of 400 °C and varying bond forces, of minimum 10 dies, determined by pull test measurements.

Table 1: Description and bonding area of three different types of bond frames.

Frame name	Description	Bonding area (mm^2)
F100	Square frame of width 100 µm and outer dimensions of 3 × 3 mm	1.16
F200	Square frame of width 200 µm and outer dimensions of 3 × 3 mm	2.24
F200R	Square frame with rounded corners of width 200 µm and outer dimensions of 3 × 3 mm	2.14

Table 2: Recipes of all 7 bonded laminates at different temperature and bond forces, all bonded for 60 minutes.

Laminate ID	Bonding Temperature (°C)	Bond Force (kN)
1	400	18
2	450	18
3	550	18
4	400	36
5	450	36
6	550	36
7	400	60

BIOGRAPHY OF AUTHORS

- Nishant Malik graduated from Amity University in Noida, India in 2011 after receiving a Master's degree in Nanotechnology. He is currently working towards the doctorate in physics from University of Oslo, Norway. He is working in collaboration with a company having research-based expertise in microsystems, SINTEF ICT. His current interests include MEMS packaging and testing. Nishant Malik is the corresponding author and can be contacted at: nishant.malik@smn.uio.no .

- Dr. Kari Schjølberg-Henriksen (1972) received her M.Sc. degree in physics from the Norwegian University of Science and Technology (NTNU) in Trondheim in 1997 and her Ph.D. degree in physical electronics from the University of Oslo, Norway, in 2003. Her thesis is entitled "Degradation of SiO2 caused by anodic and plasma activated wafer bonding". She has been employed by the research foundation SINTEF (Norway) since 1997, working in silicon process development and manufacturing of silicon-based sensors and actuators. Her research interests include wafer bonding and the Si-SiO2 system.

- Erik Poppe (1971) received his M.Sc degree in Physic from the Norwegian University of Science and Technology (NTNU) in Trondheim in 1995. He joined the Dept. of Electrical Engineering at NTNU for a research fellow position in 1996, where he worked with design and fabrication of III-V based mid-infrared semiconductor lasers. In 2001, he started working for the Dept. of Microsystems and Nanotechnology at SINTEF ICT, where he currently holds a Senior Research position and is Production Manager for the cleanroom.

- Dr. Maaike M.V. Taklo received her M.Sc. degree in physics from the Norwegian University of Science and Technology (NTNU) in Trondheim in 1997 and her Ph.D. degree in physical electronics from the University of Oslo, Norway, in 2002 for her thesis entitled "Wafer bonding for MEMS". She was employed by AME AS working with qualification of radiation sensors from 1997 until 1998 when she became employed by SINTEF ICT in Oslo, Norway, at the Department of Microsystems and Nanotechnology. Presently she is employed by SINTEF ICT at the Department of Instrumentation which she joined in 2010. She is Research Manager for "Advanced Packaging and Interconnects" within this department.

- Terje Finstad received a Cand. Real. degree in semiconductor physics from Department of Physics, University of Oslo in 1972 with a thesis on ion implantation in GaAs. He received his dr. Philos on Silicides in 1980 from the University of Oslo. He has been a Professor in Physical Electronics at the University of Oslo since 1985. His current research interests include rare earth doping of films for energy conversion and lightening, photovoltaic materials , transport in thermoelectrics, defects in oxides and and process developments. He is elected member of the Bohmische Physical Society for contributions to the field of ion-solid interactions.